ID 1508

3D FINITE ELEMENT SIMULATION ON PART DISTORTION OF CURVED COMPOSITE STRUCTURES

Y. Ding [1] , W. K. Chiu [1] and X. L. Liu [2]

[1]*Department of Mechanical Engineering, Monash University, Clayton, Melbourne, VIC. 3800, Australia*

[2] *Cooperative Research Centre for Advanced Composite Structures (CRC-ACS) 506 Lorimer Street, Fishermans Bend, VIC. 3207, Australia*

SUMMARY: In this paper, a 3-D Finite Element Analysis procedure was developed to predict the part distortion of curved shell composite structures. The results of the FE analysis were evaluated together with the results of the analytical study and experimental investigation conducted by Jain [1]. It was concluded, based on these results, that the FE model gives more accurate results than the analytical model, particularly for thicker composite shells. The effects of the corner radius, shell thickness, and lay-up sequence of the laminates on the warpage were discussed. Further discussion was also made in comparing to the experimental results reported by Radford and Rennick [2]

KEYWORDS: Part distortion, "Spring-in", Anisotropy, Composite, Laminate, FEA.

INTRODUCTION

The advantages of fiber reinforced composite structures, including their lightweight, design flexibility, corrosion resistance and noise transmission reduction compared to those made from conventional materials, have increasingly attracted a wide range of applications from aerospace to automotive industries. However, one of the problems that hinder their widespread industrial implementation is the warpage of complex composite structures, which occurs during manufacturing process. The manufacturing distortion of composite structures is caused by a number of sources. Anisotropy is the most commonly recognized source of distortion during manufacturing of laminated composite structures. Other sources such as fiber volume fraction gradient [3,4] and part/tool interactions [5,6] also have their contributions to warpage.

Since anisotropy is the most dominant source of distortion, much research effort has been devoted to address this problem. During manufacturing of curved or angled composite structures, the enclosed angle of such a structure tends to reduce after it cools down from the cure temperature. This shape change in a curved structure is illustrated in Figure 1. This phenomenon is referred to as "Spring-in". Unlike isotropic materials, there are significant differences between the coefficient of thermal expansion (CTE) in the through thickness direction and the CTE in the fiber direction in laminated composite structures. These different CTEs result in a differential out-of-plane contraction compared to the in-plane contraction during cooling down of the composite structure from curing temperature [7-8]. Resin cure shrinkage has also been suggested to form a part in "Spring-in" due to the inherent anisotropy of resin content in different directions [13, 4, 14]. Other factors such as lay-up sequence of laminates, radius and thickness of shell structures, tooling angles and materials etc. in relation to distortion have also been reported [1-2].

"Spring-in" has been a major problem for manufacturers. To satisfy the requirement of part precision, very often tooling has to be modified in order to compensate for such a distortion. At present, this re-tooling process is mainly conducted by trial-and-error and on the basis of past experience. The cost involved in such an iterative tooling modification process can be expensive. In order to fully understand manufacturing distortion and eventually lead to a cost-

effective solution to the problem, some recent research effort has been focused on modeling the phenomenon of "Spring-in". Jain [1] developed an analytical model of "Spring-in" using a solid mechanics approach to study the effects of radius-to-thickness of curved structures, lay-up sequence of laminates, and tooling angles on "Spring-in". Jain also conducted a series of experimental work using three different laminates and compared his analytical results to the experimentally measured data. However, Jain's model does not take into account of the interaction between tooling and laminates during cure and the through-thickness material property variations, such as volume fraction gradients, which generally occur in autoclave cures.

Using a laser rotation technique, Radford and Rennick [2] conducted an experimental investigation during which "Spring-in" of autoclave-cured composites was measured at temperatures ranging from 24 ^{o}C to 178 ^{o}C. According to their experimental results, Radford and Rennick suggested that three mechanisms, anisotropy, material property gradients (resulted from the matrix bridging or resin rich layers) and stress gradients (resulted from the part/tool interaction), contribute to the final manufacturing distortion, and the portion of distortion caused by each mechanism can be further separated into a thermoelastic and non-thermoelastic component. The thermoelastic component is temperature and humidity sensitive, thus, is reversible. The non-thermoelastic component is related to stress that is induced isothermally during the curing process, thus, is irreversible. This theory is able to explain some seemly contradictory findings reported previously.

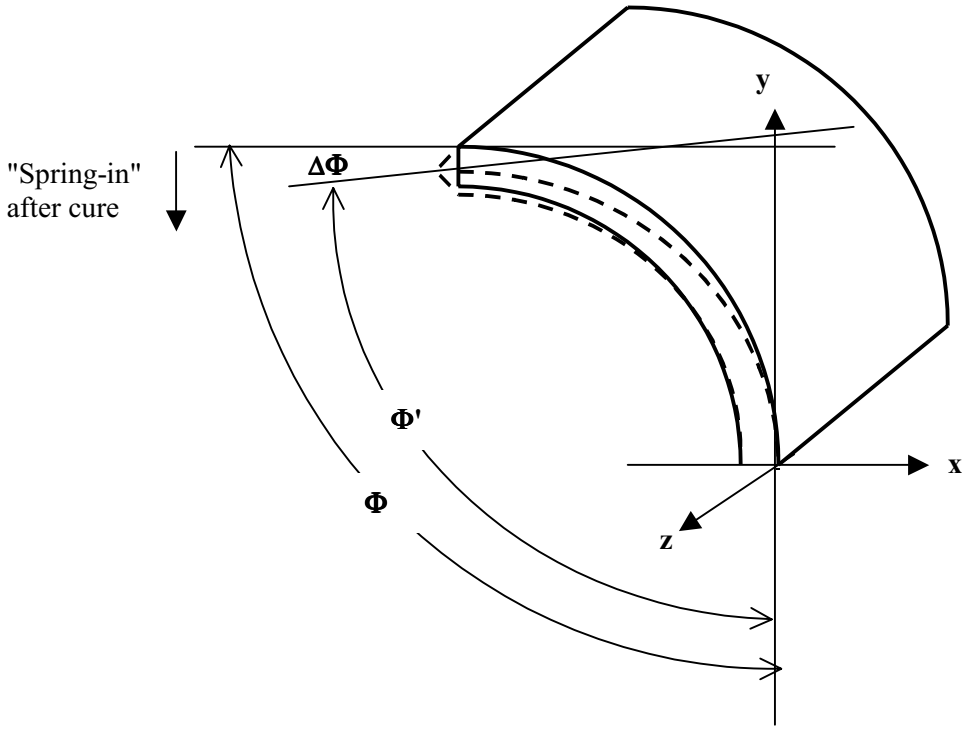

Figure 1. "Spring-in" of an angled composite shell structure.

Since multiple factors are responsible for manufacturing distortion of curved composite structures, it is difficult to take all of them into account in an analytical model. Moreover, Radford and Rennick described the total distortion using a single equation by grouping all these factors into five terms, three out of the five are characteristic descriptions only. Considerable research resources are required to obtain empirical solutions for these three sections. As an alternative, the Finite Element Method was employed by the authors to predict manufacturing distortion of curved composite structures. In this report, the procedure of the

three-dimensional FE model is described. The predicted "Spring-in" of curved laminate shell structures are presented and discussed. These results will be compared with the analytical and experimental results presented by Jain [1], Radford and Rennick [2].

THE FE MODEL

As shown in Figure 1, after cure, the enclosed angle of a composite shell $\boldsymbol{\Phi}$ is reduced to $\boldsymbol{\Phi}'$, which results in $\boldsymbol{\Delta\Phi}$ as the angle of "Spring-in". Using $\boldsymbol{R}$ as the mid-plane radius and $\boldsymbol{h}$ as the thickness of the shell, a series of curved composite structures were modeled with geometry ranging from $R/h = 0.6 \sim 20$. The enclosed angle $\boldsymbol{\Phi}$ was also modeled ranging from 45^o to 135^o. Figure 2 shows the FE models for the thickest shell of $R/h = 0.6$ and thinnest shell of $R/h = 20$. In these models, 3-D solid composite elements were used. Such an element allows the element properties be specified in both plane and through-thickness directions. By assuming that "Spring-in" is the result of the difference between CTEs in the through-thickness direction and in the fiber direction, the "spring-in" due to the differences in CTEs was predicted by the thermal stress analysis considering cooling down from the curing temperature. The effect of the resin cure shrinkage was accounted for by inserting the equivalent initial stresses to the composite elements in the FE models. The initial stresses were calculated from initial strains using the concept of macromechanics of laminate [9]. These initial strains were the results of the volumetric resin cure shrinkage that was estimated as 1.5 percent based on the fact that the resin shrinkage due to polymerisation reaction is typically about 1-2 percent. Furthermore, the effects of the radius of the curved composite structures, the thickness of the shell, the lay-up sequence of the laminates and the enclosed angles on "Spring-in" were also investigated and analysed.

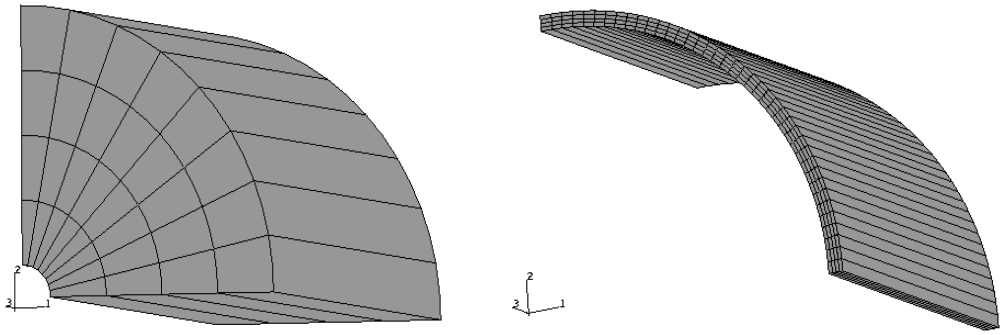

Figure 2**.** Models for the thickest shell of R/h = 0.6 and thinnest shell of R/h = 20, where h=1.6mm.

Three composite material systems used in Jain's study [1] were adopted in the present FE modeling. They were Fiberite T300/934 carbon/epoxy unidirectional laminate, plain-weave carbon/epoxy laminate, and Giba Geigy unidirectional carbon/epoxy RTM laminate. Properties of these composite systems are listed in Tables 1, 2 and 3 respectively, where the mechanical properties were estimated from the properties of the fibers and matrices. Also listed in the tables are the equivalent initial strains and stresses evaluated for the 1.5 percent of chemical volume shrinkage.

RESULTS AND DISCUSSION

Definition of "Spring-in"

Figure 3 shows the "Spring-in" of an angled composite shell by plotting its both original and displaced forms after the shell was cooled down from the cure temperature to the ambient temperature. In this case, the material was Fiberite T300/934 carbon/epoxy unidirectional

laminate and the displacement in the figure was magnified by a factor of 12. The degree of "Spring-in", $\Delta\Phi$, was calculated from the displacements of the lines along the unrestrained end at the inner and outer surfaces of the shell using one of the following equation (refer to Figure 1):

Table 1. Properties of Fiberite T300/934 carbon/epoxy unidirectional laminate

E_{11} (GPa)	E_{22} (GPa)	E_{33} (GPa)	G_{12} (GPa)	G_{13} (GPa)	G_{23} (GPa)
150.76	7.93	7.93	3.7	3.7	3.05
ν_{12}	ν_{13}	ν_{23}	ν_{21}	ν_{31}	ν_{32}
0.2525	0.2525	0.3	0.01328	0.01328	0.3
α_1 (/^{o}C)	α_2 (/^{o}C)	α_3 (/^{o}C)	**Ply thickness**		
-0.8×10^{-6}	27.62×10^{-6}	27.62×10^{-6}	0.2 mm		
ε_1^c	ε_2^c	ε_3^c	$\sigma_1^{ini.}$ (GPa)	$\sigma_2^{ini.}$ (GPa)	$\sigma_3^{ini.}$ (GPa)
-0.125×10^{-3}	-0.7056×10^{-3}	-0.7056×10^{-3}	-5.98×10^{-2}	-8.11×10^{-2}	-8.22×10^{-2}

Table 2. Properties of plain-weave carbon/epoxy 0^o laminate

E_{11} (GPa)	E_{22} (GPa)	E_{33} (GPa)	G_{12} (GPa)	G_{13} (GPa)	G_{23} (GPa)
80.05	80.05	8.68	4.0	3.465	3.465
ν_{12}	ν_{13}	ν_{23}	ν_{21}	ν_{31}	ν_{32}
0.0275	0.2525	0.2525	0.0275	0.02738	0.02738
α_1 (/^{o}C)	α_2 (/^{o}C)	α_3 (/^{o}C)	**Ply thickness**		
1.73×10^{-6}	1.73×10^{-6}	44.42×10^{-6}	0.19 mm		
ε_1^c	ε_2^c	ε_3^c	$\sigma_1^{ini.}$ (GPa)	$\sigma_2^{ini.}$ (GPa)	$\sigma_3^{ini.}$ (GPa)
-0.06×10^{-2}	-0.06×10^{-2}	-0.9×10^{-2}	-7.07×10^{-2}	-2.75×10^{-2}	-8.20×10^{-2}

Table 3**.** Properties of unidirectional carbon/epoxy RTM laminate

E_{11} (GPa)	E_{22} (GPa)	E_{33} (GPa)	G_{12} (GPa)	G_{13} (GPa)	G_{23} (GPa)
106.3	16.67	5.44	2.43	2.43	2.13
ν_{12}	ν_{13}	ν_{23}	ν_{21}	ν_{31}	ν_{32}
0.09	0.275	0.275	0.0141	0.0140	0.0897
α_1 (/^{o}C)	α_2 (/^{o}C)	α_3 (/^{o}C)	**Ply thickness**		
0.145×10^{-6}	13.0×10^{-6}	53.25×10^{-6}	0.25 mm		
ε_1^c	ε_2^c	ε_3^c	$\sigma_1^{ini.}$ (GPa)	$\sigma_2^{ini.}$ (GPa)	$\sigma_3^{ini.}$ (GPa)
-0.0317×10^{-2}	-0.316×10^{-2}	-1.21×10^{-2}	-6.05×10^{-2}	-3.72×10^{-2}	-7.33×10^{-2}

$$\Delta\Phi = \arctan\left(-\frac{-h\cdot|\sin(90-\Phi)|+u_{out-X}-u_{in-X}}{h\cdot|\cos(90-\Phi)|+u_{out-Y}-u_{in-Y}}\right)-(90-\Phi),\ 0<\Phi\le 90$$

$$\Delta\Phi = \arctan\left(\frac{h\cdot|\sin(180-\Phi)|+u_{out-Y}-u_{in-Y}}{h\cdot|\cos(180-\Phi)|+u_{out-X}-u_{in-X}}\right)-(180-\Phi),\ 90<\Phi<180 \quad (1)$$

where **Φ** is the enclosed angle of the composite shell (see Figure 1), ***h*** is the thickness of the shell. $u_{out\text{-}X}$ and $u_{in\text{-}X}$ are the displacements at the inner and outer surfaces of the unrestrained end of the shell along the X-axis direction, while $u_{out\text{-}Y}$ and $u_{in\text{-}Y}$ are the corresponding displacements along the Y-axis direction, respectively.

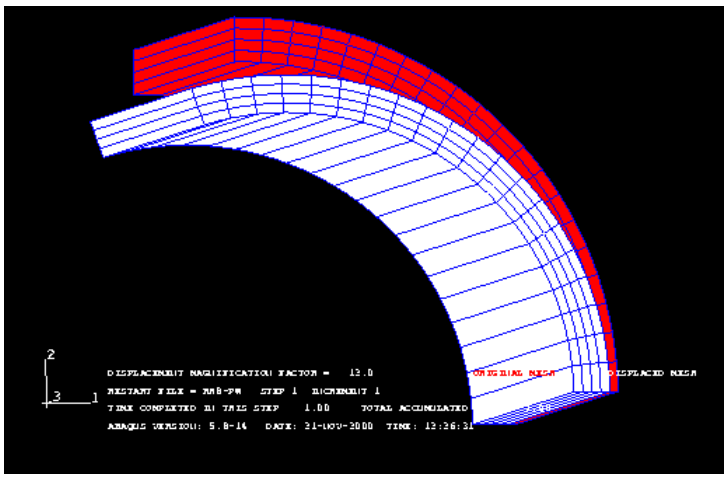

Figure 3. "Spring-in" modeling

Effect of Mid-plane Radius

In order to study the effect of mid-plane radius on "Spring-in", a series of composite (Fiberite T300/934 carbon/epoxy unidirectional tape) shells with various radii were modeled, and the results are summarized in Figure 4. For all cases presented in the figure, the enclosed angle Φ was 90°, and the lay-up sequence was $[90/0/90/0]_s$. The mid-plane radius R varied from 0.96mm to 32mm, which gives the radius-to-thickness ratio $R/h = 0.6 \sim 20$. For the thermal loading, the temperature increment, ΔT, was set to -156 °C, the same as that in Jain's investigation. For each geometry case, the "Spring-in" effect was simulated considering both situations with and without resin chemical shrinkage.

From Figure 4, it can be clearly seen that, when $R/h \geq 1$ (i.e. $R \geq h$), the predicted "Spring- in" by FEM agreed very well with Jain's analytical results for both cases with and without resin chemical shrinkage. However, when R/h <1 (i.e. $R<h$), the FEM results showed a decrease of "Spring-in" with reducing the ratio, while Jain's analytical results showed an increase of "Spring-in". There were no experimental results available to address this discrepancy in the results. However, it can be argued that for a given radius, the thicker shells should have less "Spring-in" as they have higher bending stiffness as compared to the thinner ones. It is also expected that for a given thickness, when R and hence R/h approaches 0, there should be no "Spring-in". Such a trend is only predicted by the present results. In Jain's analytical model the transverse normal stress (i.e. the stress in the shell thickness direction) was assumed to be zero everywhere, thus, the problem was simplified into 2-D shell analysis. When $R/h<1$, thickness becomes the dominant dimension, therefore, this assumption may not be valid. Nevertheless, since there are very few composite structures with geometry in the range of $R/h<1$, the results in this geometrical range are of less practical significance.

According to the "Spring-in" model developed by Radford [10], the radius does not contribute to either thermoelastic or non-thermoelastic distortion that are based solely on the anisotropy mechanism. However, both the FEM and the analytical results presented in Figure 4 show that this is true only for curved shells of $R/h \geq 1$.

It should also be noted that the effect of the radius on distortion is still a subject of more research. The experimental results published recently by Radford and Rennick [2] showed that the non-thermoelastic portion of distortion was radius dependent. The larger the radius was, the less distortion was measured. Their results were apparently contradictory to the work done by some other researchers. Nelson, et al [8], investigated distortion as the result of part/tool interaction and suggested that larger radius result in greater distortion. Obviously, further research needs to be done for a complete understanding of the effect of radius on distortion.

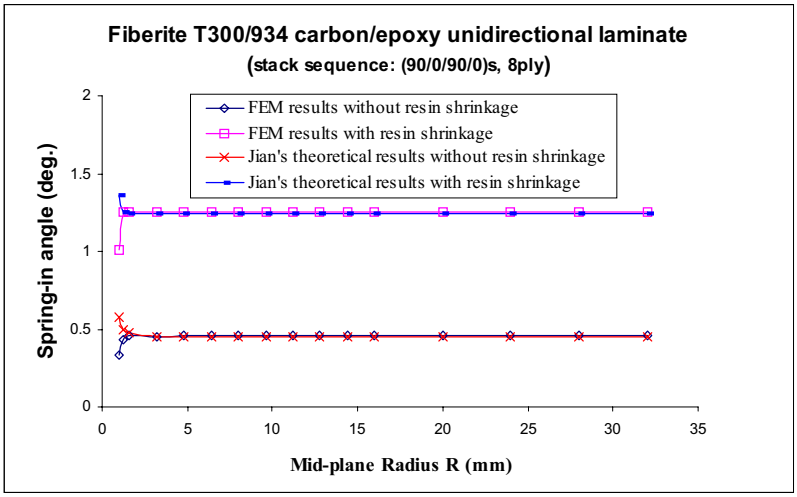

Figure 4. "Spring-in" versus mid-plane radius, R, for a cross ply [90/0/90/0]s unidirectional laminate shells with enclosed angle of 90^{o}.

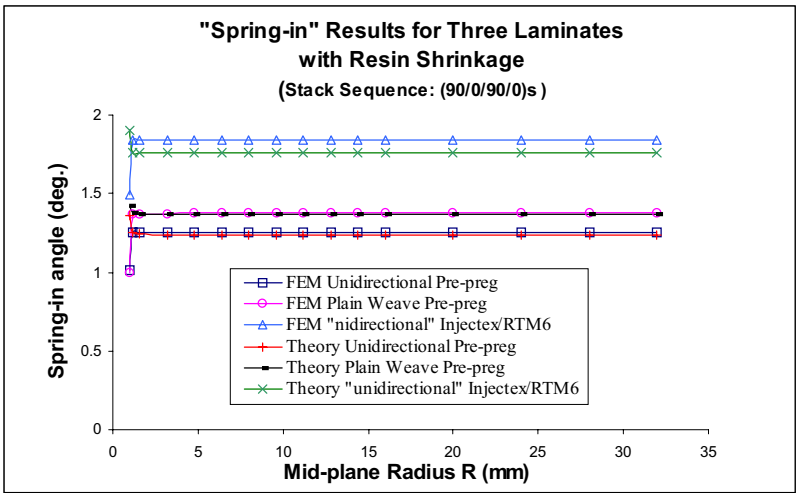

Figure 5. "Spring-in" verses mid-plane radius, R, for a cross ply laminates of h=1.6mm.

Effect of Lay-up Sequence

Finite element analyses were conducted to investigate the effect of lay-up sequence on spring-in. The material used for this phase of work was Fiberite T300/934 unidirectional pre-preg tape. The enclosed angle was 90^{o} and the shell inner radius is 3mm for seven laminates with different lay-up sequences, of which the first five laminates were 4 layers (i.e. the thickness

h=1mm) and the last two were 8 layers (*h=2mm*). The results were compared to Jain's analytical solutions and experimental results from the parts made on male and female tools and shown in Figure 6.

The results compared in Figure 6 show that both the analytical and FEM predictions agreed reasonably well with the experimentally measured data, with the exceptions being the results from two lay-up sequences of $[45/-45]_s$ and $[60/-60]_s$. The apparent disagreement in Figure 6 can be explained as follows. The results of both analytical and FEM models were only the portions of distortion resulted by anisotropy mechanism, while the experimentally measured "Spring-in" was the total distortion that included the portions of distortion due to other effects, such as the material property gradient and part/tool interaction. According to the microscopic examination on the cross sections of these specimens conducted by Jain, the effect of material property gradients on distortions of these specimens can be assumed to be minimum except the shells with $[45/-45]_s$ and $[60/-60]_s$ lay-up sequences produced on female-tooling, on which severe material property gradients was observed. Disregarding the experimental data measured from [45/-45]s and [60/-60]s shells produced by the female-tooling in Figure 6, all the results in these two figures show the same trend that an increase in the ply orientation angle resulted in increase of "spring-in". This is because that the increasing the lay-up angle results in a higher anisotropy between the circumferential direction and the through thickness direction. It was also observed that, except the [0/0]s lay-up, the experimental results from the male tooling were generally less than the results from both the FE and analytical models, while the experimental results from the female tooling were generally greater than the results from the other two. Since that the FE and the analytical models only considered part distortion resulted by anisotropy, the differences between the predicted "Spring-in" by these two models and the experimental results should be due to other effects, such as part/tool interaction and material property gradient resulted from resin rich layers or matrix bridging. According to Jain's microscopic examination on the cross-section of these specimens, no resin rich layers or matrix bridging were found in them, except the [45/-45]s and [60/-60]s lay-ups. Therefore, the differences between the experimental and the predicted data in Figure 6 should be the effect of part/tool interaction mainly. Furthermore, for the last two sets of 8-ply composites in Figures 6, both experimental and FE results show a variation in "Spring-in".

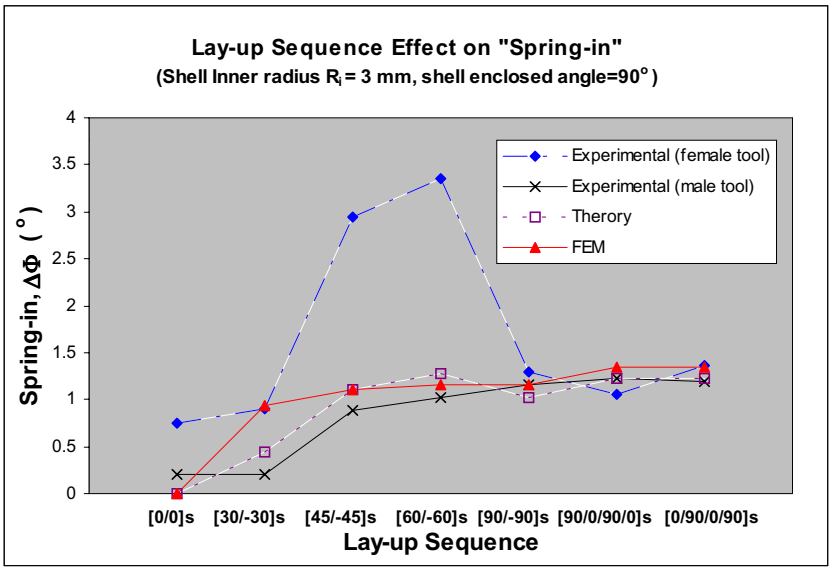

Figure 6. Effect of lay-up on "spring-in" of angled composite parts.

Effect of Enclosed Angle

The effect of enclosed angle on "Spring-in" was investigated using the plain-weaver Fabric pre-preg laminates. The detail of the material property can be found in Table 2. The mid-plane radius of all the investigated angled shells was 2mm. There were three different ply orientation groups: 0^o plies only, 45^o plies only, and combination of 0^o and 45^o plies. Each group had three different thickness of shells consisted of 4, 6 and 10 plies. The enclosed angle of each laminate varied from 45^o to 135^o. Figures 7, 8 and 9 show the comparisons between the experimental, analytical and FEM results for $[0/0]_s$, $[0/45/0]_s$ and $[45/45/45//45/45]_s$, respectively. The experimental, analytical and FE spring-in results for all nine angled parts considered were listed in Table 4.

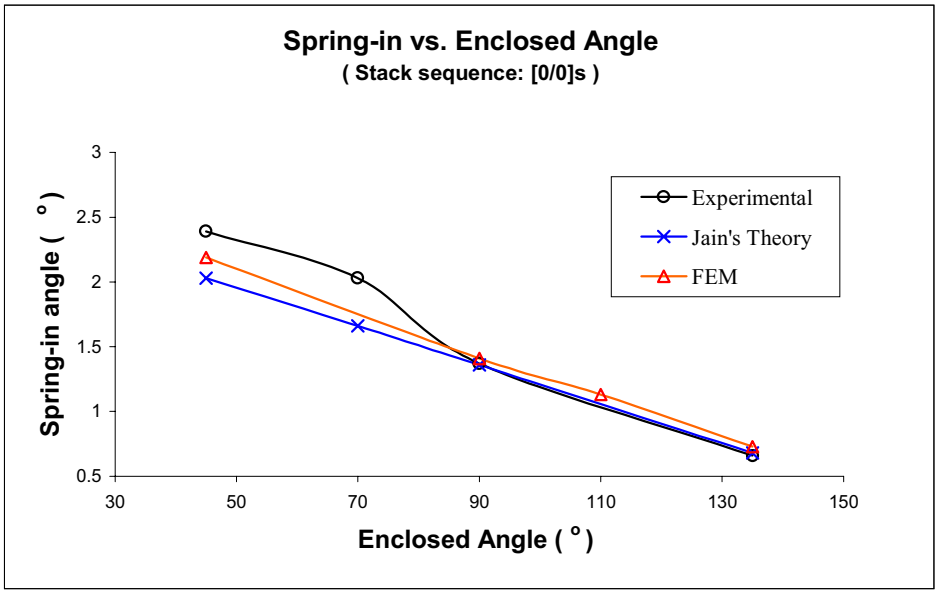

Figure 7. Effect of enclosed angle on "Spring-in" for $[0/0]_s$ plain-weave angled shell.

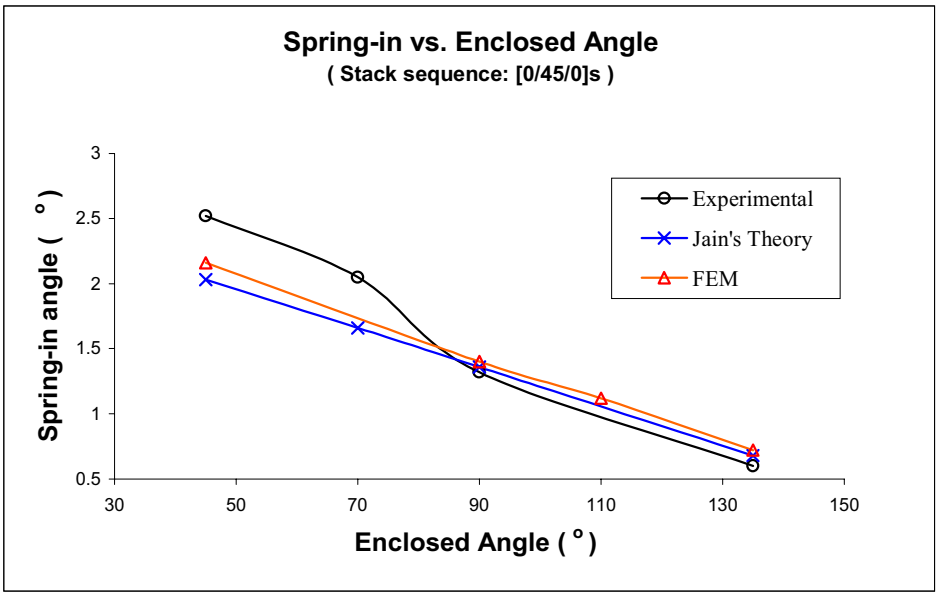

Figure 8**.** Effect of the enclosed angle on "Spring-in" for $[0/45/0]_s$ plain-weave angled shell.

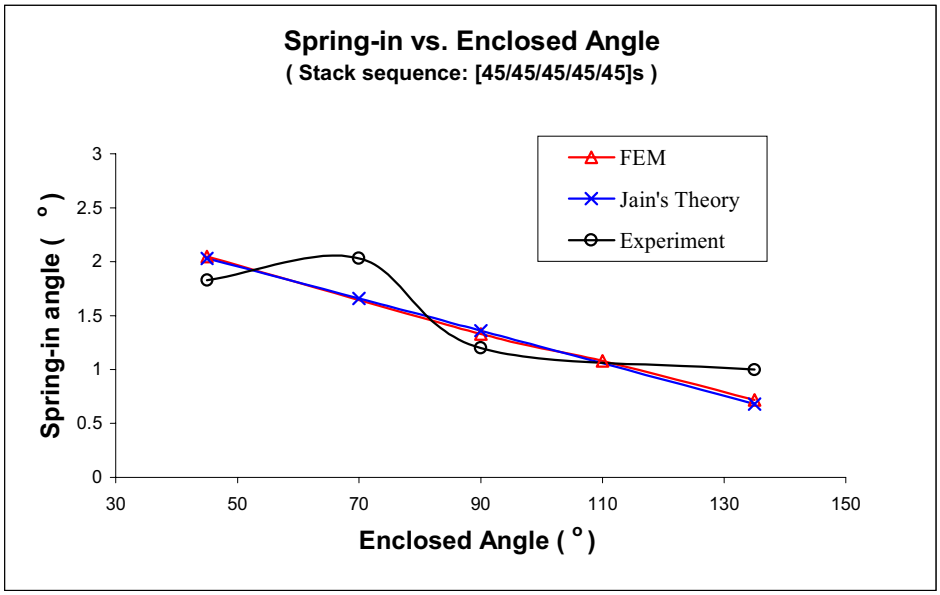

Figure 9. Effect of the enclosed angle on "Spring-in" for $[45/45/45/45/45]_s$ plain-weave angled shell.

Table 4. Degrees of "Spring-in" of plain-weave pre-preg angled shells

Lay-up	Experimental				Analytical				FEM			
	45 °	*70 °*	*90 °*	*135 °*	*45 °*	*70 °*	*90 °*	*135 °*	*45 °*	*90 °*	*110 °*	*135 °*
[0/0]s	2.39	2.03	1.37	0.66	2.03	1.66	1.36	0.68	2.19	1.41	1.13	0.73
[0/0/0]s	2.0	2.34	1.74	0.95	2.03	1.66	1.36	0.68	2.19	1.41	1.13	0.73
[0/0/0/0/0]s	1.89	1.97	1.26	0.86	2.03	1.66	1.36	0.68	2.19	1.41	1.13	0.73
[45/45]s	2.25	2.17	1.41	0.69	2.03	1.66	1.36	0.68	2.06	1.33	1.06	0.70
[45/45/45]s	1.93	2.08	1.48	0.79	2.03	1.66	1.36	0.68	2.06	1.33	1.07	0.71
[45/45/45/45/45]s	1.83	2.03	1.20	1.00	2.03	1.66	1.36	0.68	2.05	1.33	1.08	0.72
[0/45]s	1.96	1.98	1.36	0.58	2.03	1.66	1.36	0.68	2.15	1.39	1.11	0.715
[0/45/0]s	2.52	2.05	1.32	0.60	2.03	1.66	1.36	0.68	2.16	1.40	1.12	0.722
[0/45/0/45/0]s	2.02	1.84	1.33	0.91	2.03	1.66	1.36	0.68	2.16	1.39	1.12	0.723

The Figures and Table presented above indicated that there was a reasonably good agreement between the FE, analytical and experimental "Spring-in" results. In particular, it was shown that an increase in the enclosed angle, Φ, resulted in decrease of "Spring-in". This was also supported by the experimental results reported by Radford and Rennnick [2] and the prediction of Nelson et al. [12]. This can also be explained due to the definition of the enclosed angle. A smaller Φ represents a longer circumference of a shell. This will result in a larger contraction in the circumferential direction, hence a larger degree of "Spring-in".

It can also be seen from Table 4 that the same "Spring-in" was predicted by Jain's analytical model for all the nine different lay-ups. The "Spring-in" predicted by the FEM model varied with different lay-ups. Even in the same orientation group, FEM prediction for "spring-in" varied slightly with different thickness, except the 0^o-orientation group. The variation in the "Spring-in" predicted by the FEM prediction matches to that of the experimental data. Since the FEM model predicts "Spring-in" due to anisotropy mechanism only, the differences between the FEM results and experimental data should mainly represent the distortion components resulting from part/tool interaction.

CONCLUSIONS

This paper presents the finite element analyses for the prediction of "Spring-in" phenomenon of composite curved shells due to anisotropy mechanism. The temperature of the curved shells was varied from the curing temperature of composites to the ambient temperature. In order to compare the results of the FEM model to the analytical and experimental results reported by Jain [1], three composite materials used in Jain's investigation were also used here for the numerical simulation (see Tables 1, 2 and 3). The following conclusions can be drawn:

(1) The FEM model results agree with the analytical and experimental results;
(2) When $R \geq h$, the mid-plane radius of a curved shell has no effect on the "Spring-in" due to anisotropy mechanism;
(3) The degree of "Spring-in" increases while the ply orientation angle increases from 0^o to $|90^o|$.
(4) Increase of the enclosed angle, Φ, of an angled shell, i.e. decrease of the circumference arc, results in decrease of "Spring-in".
(5) It appears that, when the enclosed angle, Φ, is equal to or greater than 90^o, the male tooling reduces the degree of "Spring-in", while in general, the female tooling increases "Spring-in". More work is required to substantiate this condition.

REFERENCES

1. Jain, L. K., "Spring-in Modeling", a Report of Cooperative Research Centre for Advanced Composite Structures, Australia (CRC-AS), confidential.
2. Radford, D. W. and Rennick T. S., "Separating Sources of Manufacturing Distortion in Laminated Composites", Journal of Reinforced Plastics and Composites, Vol. 19, No 08/2000, 2000, 621 - 641.
3. Hahn, H. T. and Pagano, N. J., Journal of Composite Materials, 1975, 9: 91.
4. Madhukar, M. S., Kosuri, R. P., and Bowles, K. J., "Reduction of Curing Induced Fiber Stresses by Cure Cycle Optimization in Polymer Matrix Composites", Proceedings of ICCM X, 1995, 3: 157.
5. Pagliuso, S., "Warpage, a Nightmare for Composite Parts Producers", Proceedings of ICCM IV, 1982, 2: 1617.
6. Hubert, P., Johnston, A., Vaziri, R. and Pourtsartip, A., "A Two-Dimensional Finite Element Processing Model for FRP Composite Components", Proceedings of ICCM X, 1995, 3:149.
7. Radford, D. W. and Diefendorf, R. J., "Shape Instabilities in Composites Resulting from Laminate Anisotropy", Proceedings of the Fourth Japan-United States Conference on Composites Materials, Washington, D. D., 1988, p439.
8. Nelson, R. H., "Prediction of Dimensional Changes in Composite Laminates During Cure", Proceedings of 34th International SAMPE Symposium, 1989, 2397-2410.
9. Jones, R. M, Mechanics of Composite Materials, 2nd Edition, ISBN 1-56032-712-X, Edwards Brothers, Ann Arbor, MI, 1998.
10. Radford, D. W., Shape Stability in Composites, Ph.D. Thesis, Rensselaer Polytechnic Institute, 1987.